



Cytotoxicity evaluation and antimicrobial studies of starch capped water soluble copper nanoparticles

Mayur Valodkar^a, Puran Singh Rathore^a, Ravirajsinh N. Jadeja^b, Menaka Thounaojam^b, Ranjitsinh V. Devkar^b, Sonal Thakore^{a,*}

^a Department of Chemistry, Faculty of Science, The Maharaja Sayajirao University of Baroda, Vadodara 390002, Gujarat, India

^b Department of Zoology, Faculty of Science, The Maharaja Sayajirao University of Baroda, Vadodara 390002, Gujarat, India

ARTICLE INFO

Article history:

Received 16 July 2011

Received in revised form

23 November 2011

Accepted 23 November 2011

Available online 1 December 2011

Keywords:

Mouse embryonic fibroblast (3T3L1) cells

Copper nanoparticles

Cytotoxicity

Bactericidal

ABSTRACT

Water soluble monodisperse copper nanoparticles of about 10 nm diameter were prepared by microwave irradiation using starch as green capping agent. The resulting Cu–starch conjugate were characterized by FTIR and energy dispersive X-ray analysis (EDX). The study confirmed the presence of copper embedded in polysaccharide matrix. The aqueous solution of starch capped copper nanoparticles (SCuNPs) exhibited excellent bactericidal action against both gram negative and gram positive bacteria. The *in vitro* cytotoxicity evaluation of the nanoparticles was carried out using mouse embryonic fibroblast (3T3L1) cells by MTT cell viability assay, extracellular lactate dehydrogenase (LDH) release and dark field microscopy imaging. The capped nanoparticles exhibited cytotoxicity at much higher concentration compared to cupric ions. Minimum bactericidal concentration (MBC) of SCuNPs was well below the *in vitro* cytotoxic concentration. Statistical analysis demonstrated $p < 0.05$ for significant results and $p > 0.05$ for non-significant ones as compared to untreated cells. The non-cytotoxic green Cu–starch conjugate offers a rational approach towards antimicrobial application and for integration to biomedical devices.

© 2011 Elsevier B.V. All rights reserved.

1. Introduction

Nanomaterials are being reported as excellent vectors for the targeting and delivery of medicines and biological molecules [1]. Due to overuse of antibiotics and a growing problem of antibiotic resistance, nanoparticles are being researched as alternative antimicrobial agents [1,2]. The presence of nanoparticles in suspension would ensure continuous release of ions into the nutrient media. In addition to the direct effect of the nanoparticles on bacterial membrane, the bactericidal effects are also impacted by the release of metal ions in solution [3]. Furthermore, due to size reduction nanoparticles can traverse through the vasculature and localize any target organ. This potentially can lead to novel therapeutic, imaging, and biomedical applications.

Due to the strong reactivity of free electrons present on their surface, uncapped nanoparticles are very sensitive to their environmental factors such as pH, temperature, electrolytes and solvent, having the tendency to easily aggregate. A key issue for nanoparticles to be integrated with biological molecules is their surface chemistry that determines their stability, functionality and applications. The nanoparticle coating is crucial for ensuring the

biocompatibility inside the living organism, as other groups have demonstrated [4].

Considering environmental toxicity or biological hazards associated with chemical synthesis, the development of a green synthesis for nanoparticles is desired. Natural polymers (gelatin, dextran, chitosan) have been the first and probably the most frequently used for this purpose [5,6]. Nanoparticle stabilization with starch has been already reported in the past [7]. Further studies in our laboratory demonstrated that carbohydrates can act not only as stabilizer but also as a reducing agent, leading to formation of noble metal nanoparticles [8,9]. Such conjugated water soluble nanoparticles can have potential antimicrobial applications.

However, the suitability of nanomaterials in biological applications must be supported by studies of their potential toxicity, prior to development as clinically useful formulations [2]. The ions released by the nanoparticles may attach to the negatively charged bacterial cell wall and rupture it, thereby leading to protein denaturation and cell death [10]. There is also potential for multiple adverse interactions such as oxidative stress and inflammatory responses [3]. Such cellular processes may lead to cell death via cell necrosis or apoptosis (programmed cell death). Hence, there are many challenges to overcome before we can determine if the benefits outweigh the risks associated with NPs.

In this regard, silver is one of the most popularly used metals due to its inertness towards viable cells. Silver nanoparticles are

* Corresponding author. Tel.: +91 0265 2795552; fax: +91 0265 2429814.
E-mail address: chemistry2797@yahoo.com (S. Thakore).

incorporated in dental material, medical devices and implants to provide protection against possible microbial contamination [3]. Antimicrobial activity and cytotoxicity of AgNPs has been studied immensely [11–15]. Antibacterial activity of monosaccharide reduced silver colloids was found to be dependent on the size of silver particles [12]. Silver nanoparticles may attach to the surface of the cell membrane and disturb its power function such as permeability and respiration. Therefore it was reported that the binding of the particles to the bacteria depends on the surface area available for interaction. Smaller particles having the larger surface area available for interaction was observed to show superior bactericidal effect than the larger particles. *In vitro* cytotoxicity studies carried out by some researchers revealed non-toxic [7] or toxic [15] nature of AgNPs depending on the capping agent and dosage. Thus, the functional groups present on surface of nanoparticles could determine their uptake degree and toxicity [4].

In comparison with Ag, Cu nanoparticles are highly unstable, because copper is easily oxidized and hence, less studied [16,17]. Only a few studies have reported the antibacterial properties of copper nanoparticles (CuNPs) [11,18] while cytotoxicity has been studied to a very limited extent [19]. This investigation is based on the results of our previous study wherein starch stabilized copper nanoparticles exhibited interesting bactericidal action [20]. The mode of antimicrobial action of starch capped copper nanoparticles was compared with that of a well-known antibiotic ampicillin. The *in vitro* biological impact of the Cu nanoparticles at higher concentrations on mouse embryonic fibroblast (3T3L1) cells was also evaluated by various parameters. The cells were exposed to aqueous SCuNPs solution and finally examined by phase contrast microscopy. Moreover, in order to provide a clear assessment of their cytotoxicity, a comparative study, with cupric ions and uncapped nanoparticles was also performed.

2. Experimental

2.1. Materials and methods

Copper nitrate ($\text{Cu}(\text{NO}_3)_2 \cdot 3\text{H}_2\text{O}$), ascorbic acid and starch were purchased from Merck, Mumbai, India and solutions were prepared using double-distilled deionised water. For the synthesis of water soluble copper nanoparticles, starch was used as stabilizing agent and ascorbic acid as reducing agent as reported earlier [20]. However since the precursor concentration was kept high complexation with ammonia was necessary and hence two step reduction process was used. In the first step 0.3 mL of 0.1 M copper nitrate solution was added to 10 mL 1% solution of soluble starch with constant stirring. The pH of the solution was adjusted to 10 with ammonia solution. While, in the second step 0.6 mL of 10% (w/v) ascorbic acid solution was added whereby the pH decreased to 3. The mixture was stirred at room temperature wherein the color changed from blue to colorless to yellowish brown. The contents were then heated to boil in a domestic microwave oven at full power for about 45 s. Development of wine red color marked the formation of CuNPs. The Cu–starch conjugate was isolated by centrifuging at 10,000 rpm for 10 min and vacuum dried at 50 °C for 24 h.

2.2. Characterization

The absorption spectrum of the colloidal solution was recorded on Perkin–Elmer Lambda 35 UV–visible spectrophotometer after dilution and photoluminescence spectrum (PL) was obtained on JASCO spectrofluorometer. Particles size and distribution was assessed by TEM by a Philips, Holland Technai 20 model operating at 200 kV and Dynamic Light Scattering (DLS 90 Plus, Brookhaven, Holtsville, USA). The sample for TEM was prepared by putting one

drop of the suspension onto standard carbon-coated copper grids and then drying under an IR lamp for 30 min. FT-IR spectra of starch and vacuum dried Cu–starch conjugate were recorded as KBr pellet on Perkin Elmer RX1 model in the range of 4000–400 cm^{-1} . Morphology of the Cu–starch conjugate was examined by means of Jeol Scanning Electron Microscope (SEM model – JSM – 5610 LV, accelerating potential of 15 kV) attached to EDX.

2.3. Antimicrobial studies

Antibacterial activity of the nanoparticles solutions was examined against pathogenic organisms such as gram positive bacteria *S. aureus* (BB255) and gram negative bacteria *E. coli* (DH5 α) and *Salmonella typhi* (PTCC 1609). The minimal inhibitory concentration (MIC) and minimum bactericidal concentration (MBC) was determined with broth by the two fold serial dilution method [9]. Bacterial growth was determined by measuring optical density at 600 nm at regular intervals. In another experiment, to determine the mode of action of bacteria, the optical density was allowed to reach 0.4 at 600 nm. Nanoparticle solution corresponding to MIC concentration was added to the culture. Other two sets, solution devoid of nanoparticles (control) or antibiotic ampicillin (positive control) were added. Results of the experiment were compared with positive control ampicillin.

2.4. Measurement of cell viability by MTT assay

Mitochondrial MTT [3-(4,5-dimethylthiazol-2-yl)-2,5-diphenyl tetrazolium bromide] reduction assay was performed as per standard protocol to assess index of cell viability [21]. 3T3L1 cells (5.0×10^3 cells/well) were maintained in 96 well plates (Tarson India Pvt. Ltd.) for a period of 72 h in presence of SCuNPs (1 ng/mL–100 $\mu\text{g}/\text{mL}$) or vehicle. At the end of incubation period, 10 μL of MTT (5 mg/mL) was added to wells and the plates were incubated for 4 h at 37 °C. At the end of 4 h, culture media was discarded and all the wells were washed with phosphate buffer saline (Himedia Pvt. Ltd., Mumbai, India). This was followed by addition of 150 μL of DMSO and incubated for 30 min. Absorbance was read at 540 nm in ELX800 Universal Microplate Reader (Bio-Tek instruments, Inc., Winooski, VT, USA).

2.5. Measurement of cellular integrity by LDH assay

Cellular integrity was measured as the fraction of LDH released in the medium. 3T3L1 cells (5.0×10^3 cells/well) were maintained in 96 well plates for 72 h as described earlier. At the end of incubation period, supernatants of each well were collected and LDH activity in supernatant was measured by a commercially available kit (Reckon Diagnostics Ltd., Baroda, India) on Merck Microlab L 300 semi auto-analyzer. A solution of 1% Triton X-100 was used to achieve 100% cytotoxicity via cell-lysing (positive control).

$$\text{LDH leakage (\%)} = \frac{\text{experimental value} - \text{untreated control}}{\text{positive control} - \text{untreated control}} \times 100$$

The effectiveness of the nanoparticles was expressed as the therapeutic index (TI), which is defined as the amount of a therapeutic agent that causes a therapeutic effect of 50% in the population. The TI estimates the extent to which the administration of a drug is safe, and it is calculated as, $\text{TI} = \text{LD}_{50}/\text{MIC}$, where LD_{50} is the median lethal dose at which 50% of cell death occurs. In this work we used the 3T3L1 toxicity as a measure of LD_{50} which was $>100 \mu\text{g}/\text{mL}$, and the MIC value corresponding to *E. coli*, *S. aureus* and *Salmonella typhi*.

2.6. Morphological analysis of nanoparticles treated 3T3L1 cells

3T3L1 cells (1.0×10^5 cells/well) were maintained in 6-well plates (Tarson India Pvt. Ltd.) for a period of 72 h in presence of SCuNPs (50–1000 ng/mL) or vehicle. At the end of experimental period, cells were fixed in 4% paraformaldehyde for 10 min, mounted in glycerin, examined under Leica DMIL inverted microscope (200 \times) and photographed with Canon power shot S 72 digital camera.

2.7. Statistical analysis

Data was analysed for statistical significance using one way analysis of variance (ANOVA) followed by Bonferroni's multiple comparison test and results were expressed as mean \pm S.E.M. using Graph Pad Prism version 3.0 for Windows, Graph Pad Software, San Diego, CA, USA.

3. Results and discussion

Transmission electron microscope (TEM) images in Fig. 1A shows that the particles were uniform in diameter with a range of 5–12 nm with spherical shape. The larger particles with a size of about 12 nm were also observed along with few small particles of 5–7 nm diameters. The DLS analysis of SCuNPs presented in Fig. 1B showed a single distribution with peak centered at 14.9 nm. Considerable symmetry was observed in the particle size distribution profile. A higher particle size is often obtained in DLS for redispersed nanoparticles compared to TEM analysis [11]. In the present case

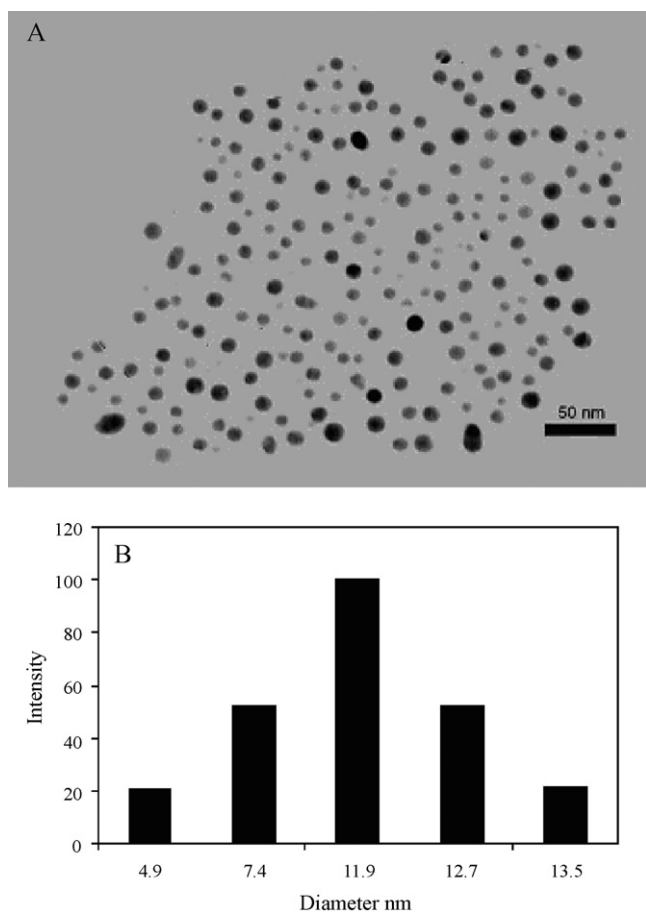


Fig. 1. (A) TEM image and (B) dynamic light scattering of starch capped copper nanoparticles (SCuNPs).

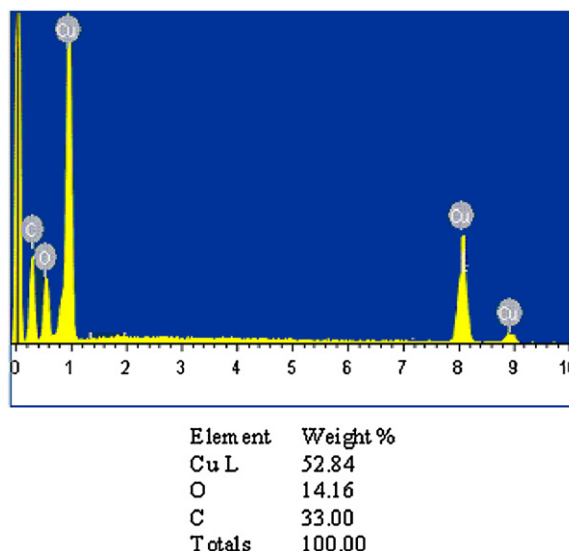


Fig. 2. Energy dispersive X-ray patterns of SCuNPs.

the results obtained by TEM and DLS are similar because of the use of same solutions in both the analysis. Also, the smaller size of the NPs in solution studies is due to effective stabilization of the nanoparticles by starch in solution.

In UV–vis spectra (supplementary data), the characteristic absorption peak at 579 nm is due to the surface plasmon resonance (SPR) of Cu colloids, which confirms the formation of Cu nanoparticles. Photoluminescence spectrum of the SCuNPs shows emission at 640 nm on excitation at 579 nm. This is assigned to the transition from excited states to d levels of the Cu nanoparticles by Sen et al. [22]. However, the Cu nanoparticles prepared by them showed absence of characteristic SPR of Cu around 580 nm, which was attributed to their much smaller diameters. Thus their excitation wavelength and hence the emission peaks are different from ours.

EDX of the Cu–starch conjugate shown in Fig. 2 confirmed the presence of copper embedded in polysaccharide matrix. No other impurities were detected in EDX profile. EDX depicts elements present in excess of 5% (w/w). Around 52 wt % of copper was present in the sample while the remaining composition is due to presence of carbon and oxygen in the polysaccharide molecules surrounding the nanoparticles [17].

The FT-IR spectra of pure starch (supplementary data) shows a peak around 3400 cm^{-1} which can be assigned to O–H stretching while the one around 2930 cm^{-1} is assigned to C–H stretching. Other peaks appeared at 1650 cm^{-1} due to C–H bending and 1015 cm^{-1} due to –C–O–C– stretching. It is seen that the peak at 1650 cm^{-1} shifts to 1605 cm^{-1} and the one at 1015 cm^{-1} shifts to 1085 cm^{-1} in the Cu–starch conjugate. The shifts observed in the spectra can be attributed to the interaction of copper with starch.

The representative photographs (Appendix B supplementary data) clearly show the zone of inhibition of *E. coli* (DH5 α) when 365 ng/mL concentration of SCuNPs was used. Similar inhibition

Table 1
MIC, MBC, LD₅₀ and TI values of SCuNPs.

Bacteria	MIC ($\mu\text{g/ml}$)	MBC ($\mu\text{g/ml}$)	Therapeutic index, TI ($\mu\text{g/ml}$)
<i>S. aureus</i>	3.2 ± 0.41	4.3 ± 0.44	$>62.5 \pm 4.26$
<i>E. coli</i>	1.6 ± 0.22	2.1 ± 0.27	$>31.25 \pm 3.71$
<i>Salmonella typhi</i>	3.6 ± 0.43	4.9 ± 0.53	$>73.57 \pm 5.14$

The LD₅₀ value was found to be $>100\text{ }\mu\text{g/ml}$.

zones were obtained in case of *S. aureus* (BB255) and *Salmonella typhi* (PTCC 1609). The MIC and MBC values shown in Table 1, indicate that the nanoparticles are more effective against *E. coli* ($r^2 = 0.62$) than *S. aureus* ($r^2 = 0.98$) and *S. typhi* ($r^2 = 0.99$). Multiple regression analysis showed more linear response with *S. aureus* and *S. typhi* compared to *E. coli*. This is due to the difference in cell wall structure between gram negative and gram positive microorganisms [14]. Due to higher negative charge on the cell-surface of gram negative bacteria the interaction with nanoparticles is stronger than gram positive bacteria. The MIC values against various MTCC and NCIM strains reported by Ruprelia et al. [11] for redispersed Cu are much higher. This was attributed to the oxide layer present on the surface. The lower MIC/MBC values in the present study may be because of the smaller size of the water soluble NPs and also due to protection from aerial oxidation offered by the biopolymer coating. Hence, it can be concluded that copper nanoparticles could be released through aqueous starch solution owing to the stable dispersion at molecular level and slow diffusion from the stabilizing medium.

Representative growth profile of bacteria in presence of SCuNPs against *E. coli* is depicted in Fig. 3A. It can be seen that the optical density of control goes on increasing with time. Whereas in samples, the growth of bacteria was observed at concentration below MIC which was reflected by increase in the optical density. As the concentration of nanoparticles increased to MIC no growth was observed in the flask causing no change in the optical density.

To understand the performance of SCuNPs an experiment was carried out as shown in Fig. 3B. The cultures were allowed to grow

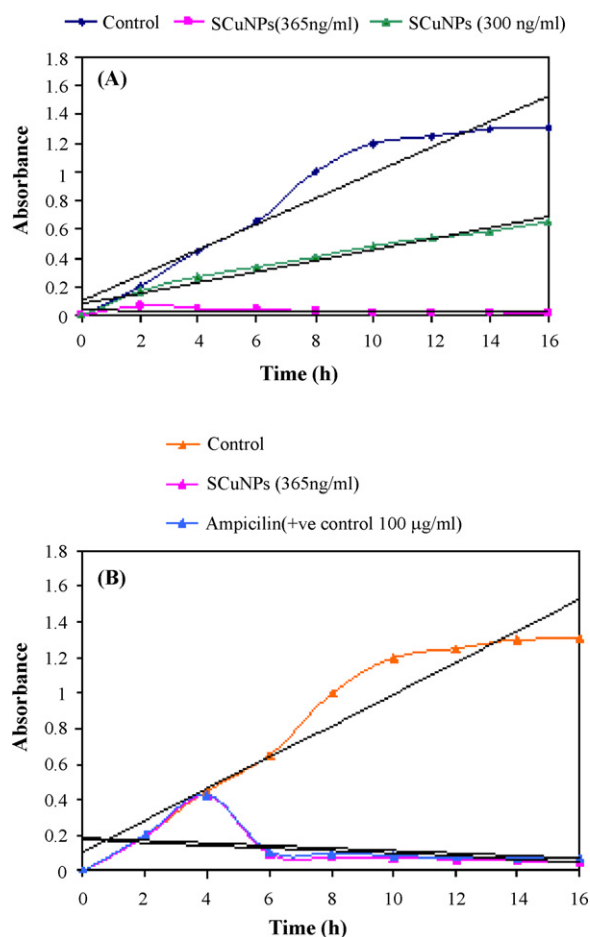


Fig. 3. (A) Growth profile of bacteria in presence and absence of nanoparticles and (B) mode of action of SCuNPs compared with ampicillin.

with *E. coli* for 3–4 h and when the optical density was observed to be around 0.4 at 600 nm three different sets were prepared. Ampicillin is a potent broad spectrum antimicrobial agent against several gram-negative rods [23]. To one of the sets 100 µg/mL of ampicillin (positive control) was added. The second set was charged with 365 ng/mL of SCuNPs which corresponds to the MIC. The third set devoid of nanoparticles/ampicillin served as the control. There was a drastic decrease in the optical density of the compound containing SCuNPs and ampicillin. The optical density almost reached zero suggesting that there were no more bacteria present in the culture. Ampicillin has the ability to lyse *E. coli* almost immediately [24]. The same effect was produced by SCuNPs at 365 ng/mL concentration.

Bactericidal effect is produced with an increase in the concentration, and cell lysis occurs because at the point of cell division there is a deformation of the cell envelope. When high ampicillin concentrations are used, cell lysis occurs before cell filamentousness is expressed [23]. The decrease in optical density is possibly associated with the cell-envelope deformation occurring at the point of cell division [23]. In another possible mechanism, the formation of hydrogen peroxide due to redox reactions between Cu^{2+} and Cu^+ at *E. coli* surface, damage the cytoplasmic membrane [25]. Copper has the potential to disrupt cell function in multiple ways, since several mechanisms acting simultaneously may reduce the ability of microorganisms to develop resistance against copper [25]. This study provides to some extent insight into the complicated antimicrobial action of copper nanoparticles. The presence of CuNPs

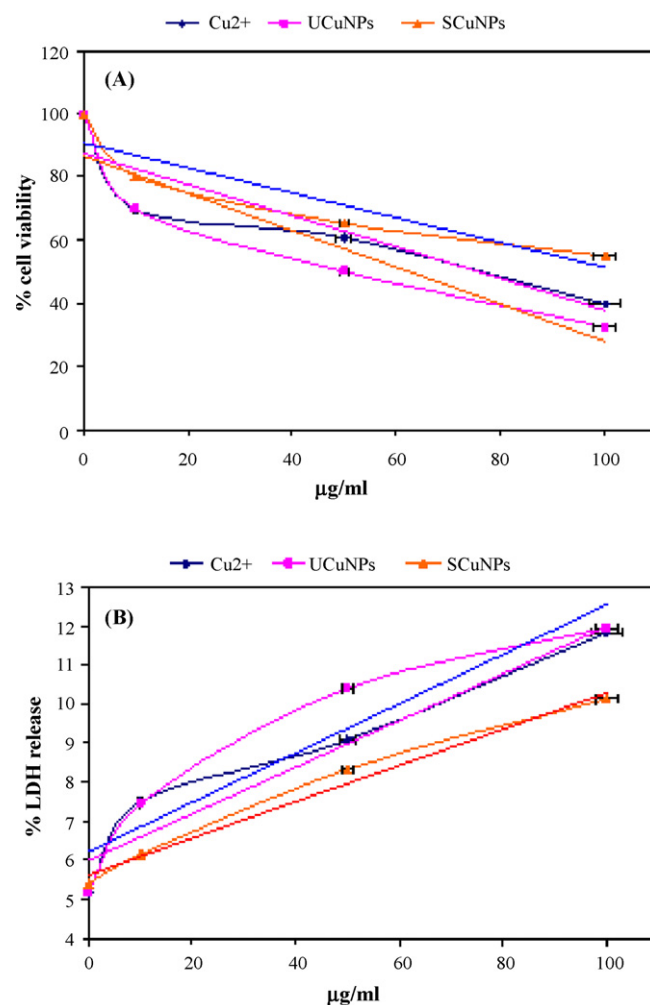


Fig. 4. Effect of SCuNPs and Cu^{2+} ions on (A) cell viability (MTT assay) and (B) cellular integrity (LDH assay) in case of mouse embryonic fibroblast (3T3L1).

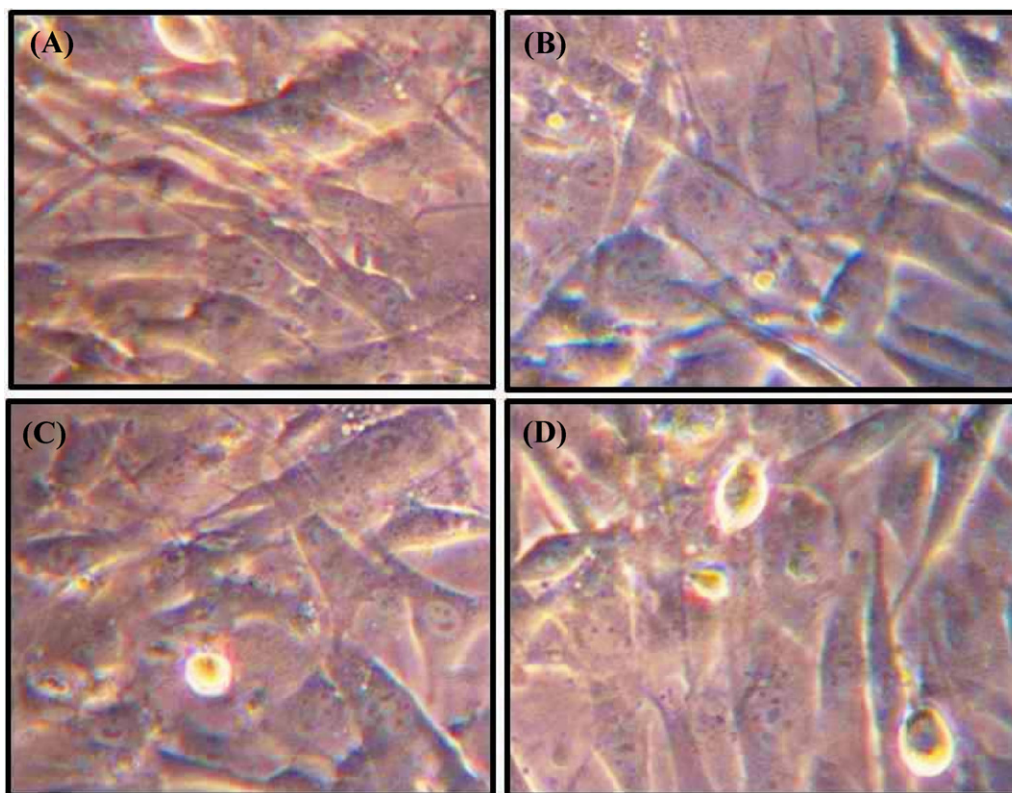


Fig. 5. Photomicrographs of mouse embryonic fibroblast (3T3L1) cells (A) untreated, treated with (B) control (C) 500 ng Cu, (D) 1000 ng Cu.

in starch suspension ensures continuous release of ions into the nutrient media. Copper ions released by the nanoparticles attach to the negatively charged bacterial cell wall and rupture it, thereby leading to protein denaturation and cell death [10]. In this study, it is assumed that SCuNPs attach to the cell wall leading to accumulation of envelope protein precursors that culminates in dissipation of the proton motive force. This proves that the SCuNPs are as potent as ampicillin against *E. coli* even at nanomolar concentrations.

Cytotoxicity depends on the shape and size of the particles [26]. While nanoparticle coating is crucial for ensuring the biocompatibility inside living organism, as other groups demonstrated [4]. The presence of additional functional groups like hydroxyl groups can lead to further bioconjugation. Travan et al. [7] demonstrated that silver nanoparticles, immobilized in biopolymeric gel matrix, can exert their antimicrobial activity by simple contact with the bacterial membrane, while they cannot be uptaken and internalized by eukaryotic cells. In a similar manner we tried to investigate the interaction of starch capped CuNPs with cell line and compared it with that of cupric ions and uncapped copper nanoparticles (UCuNPs).

Exposure of 3T3L1 cells to Cu^{2+} ions or UCuNPs resulted in significant decrement in the cell viability ($r^2 = 0.83$ and $r^2 = 0.76$) and higher LDH leakage in the dose range of 10–100 $\mu\text{g}/\text{mL}$ whereas, exposure to SCuNPs recorded identical set of changes with higher doses of 50 and 100 $\mu\text{g}/\text{mL}$ ($r^2 = 0.82$ and $r^2 = 0.87$). Multiple regression analysis revealed a non linear pattern for MTT data compared to LDH data. Dose range of 1 ng to 10 μg of SCuNPs did not register any significant cytotoxic effect (supplementary data; $r^2 = 0.7568$). Also, degree of cytotoxicity and percentage LDH leakage with doses of 50 and 100 $\mu\text{g}/\text{mL}$ were higher with Cu^{2+} ions of UCuNPs compared to SCuNPs as seen in Fig. 4. Thus the study demonstrates dose dependent cytotoxic potential of SCuNPs, that is non cytotoxic in the nanogram dose and moderately cytotoxic in the microgram doses. Comparison of SCuNPs with Cu^{2+} ions and

UCuNPs revealed that, ions are more cytotoxic than SCuNPs. This observation supports the theory of slow release of ions from starch capped nanoparticles.

From cytotoxicity experiment the LD_{50} of 3T3L1 cells exposed to SCuNPs was determined to be greater than 100 $\mu\text{g}/\text{mL}$. Moreover, these results were used to calculate the TI of SCuNPs, which measures the effectiveness of a compound. The TI value were determined to be greater than 62.5 $\mu\text{g}/\text{mL}$ in case of *E. coli* and 31.25 $\mu\text{g}/\text{mL}$ in case of *S. aureus* which is significantly high [27].

Morphology, proliferation, and differentiation are important parameters regarding cell viability, and there are many invasive methods to estimate cell viability, such as flow cytometry, colony assay, or immune staining techniques [28,29]. In this regard, visual imaging of cell population *in vitro* using low signal-to-noise ratio phase contrast microscopy can enable systematic monitoring measurements of cell quality, development and apoptosis. As previously demonstrated, the cells functions are highly correlated with their morphology [30–32]. In the present study, microscopic evaluations as seen in Fig. 5 did not reveal any significant alteration in cellular morphology upto 1000 ng/mL.

4. Conclusions

Aqueous solution of starch capped copper nanoparticles proved to be efficient non-cytotoxic bactericidal agents at nanomolar concentrations. The water solubility and biocompatible coating facilitates the direct evaluation of cytotoxicity. *In vitro* studies showed that more than 85% of the 3T3L1 cells were found to be viable, even after 20 h of time exposure which implies minimum impact on cells viability and morphology. Because of high therapeutic index the present formulation has promising antimicrobial applications. This investigation also suggests that starch capped

CuNPs have great potential for use in biomedical applications such as cellular imaging or photothermal therapy.

Acknowledgements

The authors are grateful to the U.G.C., New Delhi for financial assistance and Dr. Jayshree Pohnerkar and Mrs. Mukta Mohan, Department of Biochemistry, Faculty of Science, The M.S. University of Baroda, for antimicrobial studies.

Appendix A. Supplementary data

Supplementary data associated with this article can be found, in the online version, at doi:10.1016/j.jhazmat.2011.11.077.

References

- [1] A. Panaek, L. Kvitek, R. Prucek, M. Kolar, R. Veerova, N. Pizurova, V.K. Sharma, T.J. Nevena, R. Zboril, Silver colloid nanoparticles: synthesis, characterization and their antibacterial activity, *J. Phys. Chem. B* 110 (2006) 16248–16253.
- [2] V. Sambhy, M.M. MacBride, B.R. Peterson, A. Sen, Silver bromide nanoparticle/polymer composites: Dual action tunable antimicrobial materials, *J. Am. Chem. Soc.* 128 (2006) 9798–9808.
- [3] D. Wei, W. Sun, Q.W. Weiping, Y.Y. Yongzhong, M. Xiaoyuan, The synthesis of chitosan based silver nanoparticles and their antibacterial activity, *Carbohydr. Res.* 344 (2009) 2375–2382.
- [4] S.C. Boca, M. Potara, F. Todoras, O. Stephen, P.L. Baldeck, S. Astilean, Uptake and biological effect of chitosan-capped gold nanoparticles on Chinese hamster ovary cells, *Mater. Sci. Eng. C* 31 (2011) 184–189.
- [5] S.R. Bhattarai, K.C. Remant Bahadur, S. Aryal, N. Bhattarai, S.Y. Kim, H.K. Yi, P.H. Hwang, H.Y. Kim, Hydrophobically modified chitosan-gold nanoparticles for DNA delivery, *J. Nanopart. Res.* 10 (2008) 151–162.
- [6] S. Nath, C. Kaittanis, A. Tinkham, J.M. Perez, Dextran-coated gold nanoparticles for assessment of antimicrobial susceptibility, *Anal. Chem.* 80 (2008) 1033–1038.
- [7] A. Travan, C. Pelillo, I. Donati, E. Marsich, M. Benincasa, T. Scarpa, S. Semeraro, G. Turco, R. Gennaro, S. Paoletti, Non-cytotoxic silver nanoparticle-polysaccharide nanocomposites with antibacterial activity, *Biomacromolecules* 10 (2009) 1429–1435.
- [8] M. Valodkar, P. Sharma, D.K. Kanchan, S. Thakore, Conducting and antimicrobial properties of silver nanowire-waxy starch nanocomposites, *Int. J. Green Nanotechnol. Mater. Sci. Chem.* 2 (2010) 1–8.
- [9] M. Valodkar, A. Bhadoria, M. Mohan, J.P. Pohnerkar, S. Thakore, Morphology and antibacterial activity of carbohydrate-stabilized silver nanoparticles, *Carbohydr. Res.* 345 (2010) 1767–1773.
- [10] Y.E. Lin, R.D. Vidic, J.E. Stout, C.A. McCartney, V.L. Yu, Inactivation of mycobacterium avium by copper and silver ions, *Water. Res.* 32 (1998) 1997–2000.
- [11] J.P. Ruparelia, A.K. Chatterjee, S.P. Duttagupta, S. Mukherji, Strain specificity in antimicrobial activity of silver and copper nanoparticles, *Acta. Biomater.* 4 (2008) 707–716.
- [12] A. Panacek, L. Kvitek, R. Prucek, M. Kolar, R. Veerova, N. Pizurova, V.K. Sharma, T. Naveena, R. Zboril, Silver colloid nanoparticles: Synthesis, characterization and their antibacterial activity, *J. Phys. Chem. B* 110 (2006) 16248–16253.
- [13] K. Kawata, M. Osawa, S. Okabe, In vitro toxicity of silver nanoparticles at noncytotoxic doses to HepG2 human hepatoma cells, *Environ. Sci. Technol.* 43 (2009) 6046–6051.
- [14] D.V.M. Jun-Sung-Kim, M.S. Eunye-Kuk, K.M. Yu, M.S. Jong-Ho-Kim, B.S. Sung-Jin Park, D.V.M. Hu-Jang-Lee, D.V.M. So Hyun Kim, D.V.M. Young Kyung Park, D.V.M. Yong Ho Park, D.V.M. Cheol-Yong Hwang, Y.K. Kim, Y.S. Lee, D.H. Jeong, M.H. Cho, Antimicrobial effects of silver nanoparticles, *Nanomed. Nanotechnol.* 3 (2007) 95–101.
- [15] R. Foldbjerg, P. Olesen, M. Hougaard, D.A. Dang, H.J. Hoffmann, H. Autrup, PVP-coated silver nanoparticles and silver ions induced reactive oxygen species apoptosis and necrosis in THP-1 monocytes, *Toxicol. Lett.* 190 (2009) 156–162.
- [16] M. Abdulla-Al-Mamun, Y. Kusumoto, M. Muruganandham, Simple new synthesis of copper nanoparticles in water/acetonitrile mixed solvent and their characterization, *Mater. Lett.* 63 (2009) 2007–2009.
- [17] P.K. Khanna, S. Gaikwad, P.V. Adhyapak, N. Singh, R. Marimuthu, Synthesis and characterization of copper nanoparticles, *Mater. Lett.* 61 (2007) 4711–4714.
- [18] L. Esteban-Tejeda, F. Malpartida, A. Esteban-Cubillo, C. Pecharroman, J.S. Moya, Antibacterial and antifungal activity of a soda-lime glass containing copper nanoparticles, *Nanotechnology* 20 (2009) 505701.
- [19] M. Valodkar, P.S. Nagar, R.N. Jadeja, M. Thounaojam, R.V. Devkar, S. Thakore, Euphorbiaceae latex induced green synthesis of non-cytotoxic metallic nanoparticle solutions: a rational approach to antimicrobial applications, *Colloid. Surf. A* 84 (2011) 337–344.
- [20] M. Valodkar, S. Modi, A. Pal, S. Thakore, Synthesis and antibacterial activity of Cu, Ag and Cu–Ag alloy nanoparticles: a green approach, *Mater. Res. Bull.* 46 (2011) 384–389.
- [21] T. Mosmann, Rapid colorimetric assay for cellular growth and survival: application to proliferation and cytotoxicity assays, *J. Immunol. Methods* 65 (1983) 55–63.
- [22] O.P. Siwach, E.P. Sen, Synthesis and study of fluorescent properties of Cu nanoparticles, *J. Nanopart. Res.* 10 (2008) 107–114.
- [23] O.I. Guliy, O.V. Ignatov, L.N. Markina, V.D. Bunin, V.V. Ignatov, Action of ampicillin and kanamycin on the electrophysical characteristics of *Escherichia coli* cells, *Int. J. Environ. Anal. Chem.* 85 (2005) 981–992.
- [24] D. Greenwood, O. O'Grady, A comparison of the effects of ampicillin on *Escherichia coli* and *Pruteus mirabilis*, *J. Med. Microbiol.* 2 (1969) 435–441.
- [25] M. Raffi, S. Mehrwan, T.M. Bhatti, J.I. Akhter, A. Hameed, W. Yawar, M. Hasan, Investigations into the antibacterial behavior of copper nanoparticles against *Escherichia coli*, *Ann. Microbiol.* 60 (2010) 75–80.
- [26] B.D. Chithrani, A.A. Ghazani, W.C.W. Chan, Determining the size and shape dependence of gold nanoparticle uptake into mammalian cells, *Nano. Lett.* 6 (2006) 662–668.
- [27] F. Martinez-Gutierrez, P.L. Olive, A. Banuelos, E. Orrantia, N. Nino, E.M. Sanchez, F. Ruiz, H. Bach, Y. Av-Gay, Synthesis, characterization and evaluation of antimicrobial and cytotoxic effect of silver and titanium nanoparticles, *Nanomed. Nanotechnol.* 6 (2010) 681–688.
- [28] L. Au, D. Zheng, F. Zhou, Z.Y. Li, X. Li, Y. Xia, A quantitative study on the photothermal effect of immune gold nanocages targeted to breast cancer cells, *ACS Nano* 2 (2008) 1645–1652.
- [29] M. Mahmood, D.A. Casciano, T. Mocan, C. Iancu, Y. Xu, L. Mocan, D.T. Lancu, E. Dervishi, Cytotoxicity and biological effects of functional nanomaterials delivered to various cell lines, *J. Appl. Toxicol.* 30 (2010) 74–83.
- [30] C.R. Lee, A.J. Grodzinsky, M. Spector, Modulation of the contractile and biosynthetic activity of chondrocytes seeded in collagen-glycosaminoglycan matrices, *Tissue Eng.* 9 (2003) 25–36.
- [31] R. Oda, K. Suardita, K. Fujimoto, H. Pan, W. Yan, A. Shimazu, H. Shintani, Y. Kato, Anti-membrane-bound transferring-like protein antibodies induced cell-shape and chondrocyte differentiation in presence or absence of concanavalin A, *J. Cell. Sci.* 116 (2003) 2029–2038.
- [32] X. Huang, A. El-Sayed Mostafa, Gold nanoparticles: optical properties and implementations in cancer diagnosis and photothermal therapy, *J. Adv. Res.* 1 (2010) 13–28.